Neurological Sciences (2026) 47:892
https://doi.org/10.1007/s10072-026-09518-y

ORIGINAL ARTICLE

Is photophobia associated with the structure of the visual thalamus? A MRI morphometric study

Gianluca Coppola[1] · Antonio Di Renzo[2] · Gabriele Sebastianelli[1] · Irene Giardina[3,4] · Davide Chiffi[4] · Giada Giuliani[4] · Francesco Casillo[1] · Chiara Abagnale[1] · Lucia Ziccardi[2,6] · Andrea Pucci[5] · Maomei Song[7] · Vincenzo Parisi[2,8] · Marta Altieri[4] · Francesca Caramia[4]

Received: 19 June 2026 / Accepted: 22 October 2026
© Fondazione Società Italiana di Neurologia 2026

Abstract

Background/Objectives Photophobia is a common migraine symptom, but its cause is unknown. The posterior thalamic nuclei may directly affect ambient light discomfort. This study examined the link between photophobia and the structure and morphometry of the thalamus and its subregions, including the lateral geniculate nuclei and pulvinar subnuclei.

Methods Twenty episodic migraine patients without aura (MO) and 20 healthy controls (HCs) underwent high-resolution T1-weighted magnetic resonance imaging, diffusion tensor imaging (DTI), and full ophthalmological assessment. Scans were acquired interictally, with all patients off preventive therapy. Volumetric segmentation included the whole thalamus, lateral geniculate nuclei, and pulvinar subregions. Photophobia was rated from 0 to 10 using a visual analogue scale. Thalamic and subregion volumes served as dependent variables, while photophobia scores were independent variables in a general linear model (GLM). Bilateral thalamic DTI metrics were analyzed for relationships with volumes and photophobia scores using GLMs.

Results No statistically significant differences were observed in the overall thalamic volume or in any of its subregions and DTI metrics between MO patients and HCs ($p > 0.05$). No relationships emerged between thalamic volumes, DTI metrics, and interictal subjective photophobia scores ($p > 0.05$).

Conclusions Our results suggest a lack of association between photophobia and thalamic macro- and microstructural measures in MO patients during the interictal phase, with no significant structural or microstructural correlates identified. Further research is needed to determine whether these negative results could be extended to patients with migraine with aura or during other phases of the migraine cycle.

Keywords Visual discomfort · Freesurfer · Thalamus · Segmentation · Headache · DTI

Gianluca Coppola and Antonio Di Renzo contributed equally to this work.

✉ Gianluca Coppola
gianluca.coppola@uniroma1.it

1 Department of Medico-Surgical Sciences and Biotechnologies, Sapienza University of Rome Polo Pontino ICOT, Latina, Italy

2 Clinical and Research Center of Neurophthalmology and Genetic, IRCCS – Fondazione Bietti, Rare Diseases of the Eye, Rome, Italy

3 Department of Radiological Sciences, Oncology and Pathology, Sapienza University of Rome, Rome, Italy

4 Department of Human Neurosciences, Sapienza University of Rome, Rome, Italy

5 Neuroradiology Unit, Policlinico Umberto I, Rome, Italy

6 Department of Medicine and Health Sciences "Vincenzo Tiberio", University of Molise, Campobasso, Italy

7 Department of Neurology, Headache Center, Shanxi Provincial Laboratory for Brain Science and Neuropsychiatric Diseases, The First Hospital of Shanxi Medical University, Shanxi Medical University, Shanxi, China

8 Departmental Faculty of Medicine, UniCamillus-Saint Camillus International University of Health Sciences, Rome 00131, Italy

Published online: 22 October 2026

Introduction

Despite significant progress in migraine research, the anatomical and functional mechanisms behind canonical migraine-related symptoms, such as photophobia, remain largely unexplored [1]. Photophobia is typically characterized as an excessive sensitivity to ambient light stimuli [2] and constitutes one of the principal criteria for migraine diagnosis [3]. Although photophobia is more common during the migraine pain, patients with migraine may experience it also during the pain-free interval [4].

Evidence suggests a correlation between metabolism—assessed using visual-task-related BOLD functional MRI and glucose PET—and structural factors—including the thickness of the visual cortex's grey matter and photophobia— [5–7], alongside a calcitonin gene-related peptide (CGRP)-dependent mechanism of light sensitisation [8]. For some researchers, photophobia is facilitated by a subset of intrinsically photosensitive retinal ganglion cells that link the retina to the spinal trigeminal nucleus, as well as the lateral geniculate and pulvinar thalamic nuclei [9–12]. The triangulation of thalamic, brainstem, and retinal systems could enable the perception of the light signal as painful [13]. This evidence highlights the value of investigating whether the volume and microstructure of the thalamic nuclei also vary in response to changes in the patient's perceived levels of photophobia.

The primary aim of this study was to examine the relationship between the volumes of thalamic nuclei implicated in visual processing, such as the lateral geniculate nucleus and the pulvinar, and subjective photophobia scores on a Likert 0 to 10 scale score in patients with migraine without aura during the interictal phase. In the same patients, we also investigated whether there was a relationship between the microstructure of the thalamus and subjective interictal photophobia scores.

The Freesurfer's automated segmentation software was used to study thalamic nuclei and subnuclei volumes [14]. Additionally, we characterised the microstructural diffusion properties of the entire thalamus bilaterally using diffusion tensor imaging (DTI). Moreover, to rule out a possible influence of alterations of the anterior segment of the eye on photophobia, a comprehensive series of ophthalmological tests were conducted in all participants [2].

While previous morphometric studies have mainly focused on group-level structural differences in migraine, no study to date has specifically investigated the relationship between subjective interictal photophobia and the macro- and microstructure of visual thalamic nuclei. Therefore, this study seeks to investigate a symptom–structure relationship, rather than group differences alone, providing a novel perspective on the neurobiological basis of photophobia in migraine.

Materials and methods

We performed a secondary analysis of the data collected from our previous study, using only data from patients who also were asked for the subjective interictal photophobia level on the day of the examination [15]. Twenty patients diagnosed with episodic migraine without aura (MO) in accordance with the International Classification of Headache Disorders (ICHD III) [3] were recruited from two Headache Centers (Rome and Latina) (Table 1).

All patients maintained a headache diary provided to them upon reserving a consultation appointment for at least one month prior to their initial visit. During the first consultation, we collected detailed information on the patient's clinical characteristics, including the years from disease onset, the frequency and duration of migraine episodes each month, the intensity of headaches (assessed using a VAS scale from 0 to 10), and the days elapsed since the most recent migraine attack (Table 1). Additionally, all patients were requested to respond to the following question: In the absence of migraine pain, what is the average intensity of discomfort caused by exposure to bright light? (on a scale from 0 to 10, with 0 indicating no discomfort and 10 representing the highest level of discomfort). Exclusion criteria were the use of preventive therapy in the preceding three months, side-locked head pain, concomitant diagnosis of other primary or secondary headache types, and a history of other relevant concomitant diseases, including neurological and neuro-ophthalmological diseases.

Twenty healthy controls (HCs) of similar age and gender were recruited among medical students and healthcare practitioners for comparative investigation. Exclusion criteria

Table 1 Demographic and clinical characteristics of healthy controls (HCs) and patients with migraine without aura scanned during migraine-free intervals (MO). Data are presented as mean ± standard deviation. Group differences were tested using Student's t-test

	HCs ($n=20$)	MO ($n=20$)	Statistics
Female (n)	15	15	
Age (years)	29.00 ± 5.06	34.35 ± 11.96	t = -1.84, $p=0.08$
History of migraine (years)		17.0 ± 12.9	
Attack frequency/month (n)		6.3 ± 3.3	
Attack duration (hours)		33.2 ± 19.9	
Severity of headache (0–10)		8.3 ± 1.0	
Days from the last migraine attack (n)		5.8 ± 3.9	
MIDAS		21.0 ± 17.9	
HIT-6		61.9 ± 8.0	
ASC-12		4.1 ± 4.2	
Interictal photophobia score (0–10)		3.0 ± 1.8	

for HCs included having medical or relevant ophthalmological disorders, a personal or familial history of primary headaches or epilepsy, and not engaging in frequent drug use. Further exclusion criteria for both HCs and MOs were the existence of structural brain abnormalities on magnetic resonance imaging (MRI).

All subjects received a complete ophthalmological assessment, which included best-corrected visual acuity measurements (Snellen Equivalent), slit-lamp biomicroscopy for anterior segment evaluation, indirect ophthalmoscopy following pupil dilation (Tropicamide 1% drops) for posterior segment examination, and Goldmann applanation tonometry for intraocular pressure (IOP) measurement. All participants recruited were right-handed.

All participants were provided with a comprehensive overview of the study and granted written informed consent. The Ethical Committee of the Faculty of Medicine, Sapienza University of Rome, authorized the study protocol (Protocol No. 0295/2023, March 23, 2023).

MRI protocol

Scanning sessions were scheduled in the afternoon (4:00–7:00 p.m.). Female participants were uniformly scanned throughout the mid-cycle phase. Participants were directed to refrain from sleep deprivation and alcohol consumption the day before the scanning procedure. Caffeinated beverages were banned on the day of the scan. All patients with MO were scanned during the interictal phase, i.e., a minimum of three consecutive days before or after a migraine attack, as verified through follow-up telephone interviews. Additionally, symptomatic medication was prohibited on the day of the scan.

All participants underwent MRI on a 3-Tesla Siemens Magnetom Vida scanner, using a 32-channel head coil. High-resolution T1-weighted sagittal magnetization-prepared rapid gradient echo (MPRAGE) sequences were acquired (TR: 2300 ms, TE: 2.25 ms, 208 sagittal slices, voxel dimensions $0.8 \times 0.8 \times 0.8$ mm³, base resolution 320, field of view 256 mm, slice thickness 0.8 mm).

DTI images were obtained with a single shot echo planar image sequence with the following parameters: repetition time (TR) = 4500 ms, echo time (TE) = 78 ms, field of view (FOV) = 220 mm x 220 mm, matrix = 110×110, 2 mm x 2 mm in plane resolution, slice thickness = 2 mm, 75 continuous axial slices with no gap, 1 volume anterior to posterior (AP) phase of encoding direction b = 0 s/mm^2, b = 1000 s/mm^2, and 30 diffusion directions were isotropically distributed on a sphere where one direction lacked diffusion weighting resulting in 30 volumes of the AP phase of encoding direction and 1 volume posterior to anterior (PA) phase of encoding direction b = 0.

Imaging data processing: Thalamus subunits analysis

Thalamic segmentation was performed utilising a feature in Freesurfer 7.4.1(https://surfer.nmr.mgh.harvard.edu/fswiki/SubregionSegmentation), a Python application that delineates the thalamus into 25 nuclei, employing a probabilistic atlas derived from histology data [14].

Two experienced investigators (F.C. and I.G.) examined the thalamic segmentations of each participant, ultimately excluding those with artefacts.

We collected the volumes of the following thalamic nuclei: lateral geniculate, pulvinar anterior, pulvinar medial, pulvinar lateral, and pulvinar inferior; their volumes were calculated and recorded for each participant in the group (Fig. 1).

Diffusion Tensor Imaging (DTI)

All DTI datasets underwent visual examination by two experienced neuroradiologists (F.C. and I.G.) to detect motion artefacts, signal dropout, or heart pulsation effects. Preprocessing was conducted utilising the FMRIB Software Library (FSL, version 6.0.7; https://fsl.fmrib.ox.ac.uk/fsl) [16–18].

The top-up method was utilised to rectify susceptibility-induced distortions by employing paired b = 0 volumes obtained in anterior-posterior and posterior-anterior orientations [19].

Brain extraction was conducted with the brain extraction tool algorithm [20], whereas motion and eddy-current correction were accomplished with the eddy tool [21].

Prior to the final stage, the MRI-processed images were evaluated utilising a quality control framework [22] to detect and possibly exclude the substandard dataset.

Finally, the DTIFIT toolbox applies a diffusion tensor model to the preprocessed images to produce fractional anisotropy (FA) and mean diffusivity (MD). The whole left and right thalamic regions of interest were obtained from FSL's Harvard – Oxford Subcortical Atlas and aligned with the T1 brain-extracted MNI152 standard template. Consequently, the registration of each ROI and DTI metric was executed using the FSL Diffusion Toolbox algorithms framework for each participant [23].

The rectified non-diffusion-weighted brain-extracted volume was linearly co-registered [23, 24] with the T1 brain-extracted volume. The T1 brain-extracted volume was non-linearly co-registered with the T1 brain-extracted MNI152 standard template.

The previously assessed transformation matrices were inverted and concatenated to derive the diffusion to the T1 MNI152 standard transformation matrix, which was subsequently inverted as well.

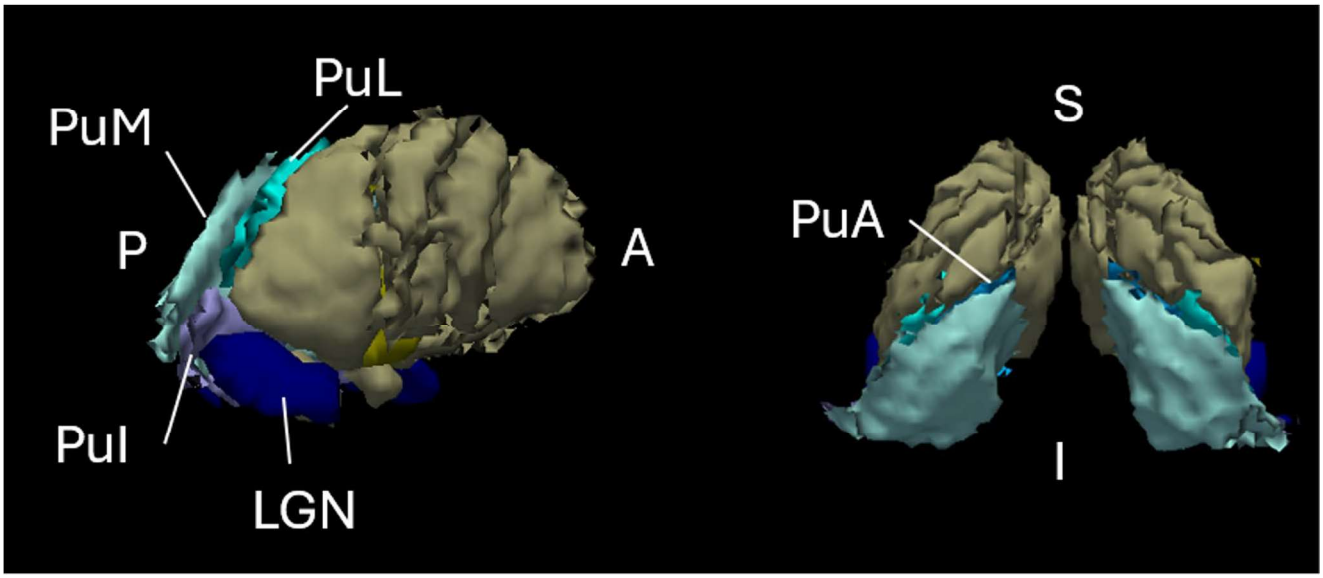


Fig. 1 Thalamic nuclei segmentation. FreeSurfer 3D rendering of thalamic nuclei in their lateral-medial (left) and caudal-rostral (right) aspects on T1-weighted multiecho MPRAGE data of a representative sample subject. Lateral geniculate nucleus (LGN), Pulvinar inferior (PuI), Pulvinar medial (PuM), Pulvinar anterior (PuA), Pulvinar lateral (PuL). P = posterior, A = anterior, s = superior, I = inferior

Finally, each thalamic region of interest was linearly co-registered utilising the corrected, non-diffusion weighted, brain-extracted volume as a reference and the T1 MNI152 standard template to the diffusion matrix, thus obtaining each region of interest in the diffusion space.

Two professional neuroradiologists (F.C. and I.G.) meticulously examined the thalamic regions of interest (ROIs) for each participant, utilising the non-diffusion weighted volume of each individual.

Statistical analysis

Descriptive and inferential statistics were used, concentrating on volumetric differences between groups and the correlation between volumes and clinical factors in the MO group. SPSS for Windows (v.21, IBM Corp.) was used for the analysis.

The total intracranial volume (TIV) of each participant was computed using Freesurfer (version 7.4.1) [25–33].

To evaluate differences in the subnuclei volumes between groups (dependent variables), we applied a general linear model (GLM) that used age and TIV as covariates (independent variables) and gender and group as factors.

Partial η^2 was evaluated for each GLM group factor.

Additionally, we applied a new GLM to assess the relationship between the volume of the MO group in each thalamic subunit (dependent variables) and interictal photophobia scores (independent variables), controlling for age and TIV as covariates and incorporating gender as a factor.

Partial η^2 were evaluated for each GLM photophobia score covariate.

The Anderson-Darling and/or Kolmogorov-Smirnov tests were performed for each model's covariates and responses to examine normality distributions.

P-value thresholds were set at 0.025 for volume discrepancies between groups of the entire thalamus (0.005 for subnuclei analyses after Bonferroni correction). The same p-value thresholds were applied to assess relationships between left and right thalamic volumes ($p < 0.025$) and their subunits ($p < 0.005$) with photophobia score.

Again, general linear models were developed to evaluate FA and MD variations between groups and relationships with photophobia score.

GLMs were made, based on ROIs DTI metrics as the dependent variable, age as a covariate, gender and group as factors, to assess any variations between groups.

Partial η^2 were evaluated for each GLM group factor.

Further GLMs were developed using ROIs DTI metrics as the dependent variable, age, left and right thalamic volumes, TIV as covariates and gender as a factor to assess any relationship between the patient's left and right thalamic volumes.

Partial η^2 were evaluated for each GLM L/R thalamic volumes covariate.

Lastly, a GLM was developed with ROIs DTI metrics as dependent variable, age and photophobia scores as covariates, and gender as a factor.

A p-value of 0.01 was chosen for ROIs' DTI metrics comparison and relationships assessment (adjusted for multiple comparisons using the Bonferroni method to address for the number of regions of interest: DTI metrics ($N = 2$) and ROIs ($N = 2$) $0.05/4 \approx 0.01$).

Results

Twenty patients with MO (15 females, mean age 29.00 ± 5.06) and 20 HCs (15 females, mean age 34.35 ± 11.96) were recorded. Participants with MO had a mean of 6.3 ± 3.3 headache days per month. The mean interictal photophobia score was 3.0 ± 1.8. Complete demographic and clinical characteristics of the participants are reported in Table 1.

None of the patients showed any relevant ophthalmological condition, and all of them had IOP < 20 mmHg and BCVA of 20/20 Snellen in both eyes.

Table 2 reports the descriptive statistics volumes of the entire thalamus and its subregions in both hemispheres. No statistically significant differences were found between MO patients and HCs in either total thalamic volume or its subregions ($p_{uncorrected} > 0.05$, Table 2).

Additionally, no significant relationships emerged between interictal photophobia scores and the total volume of the entire thalamus or its subregions ($p_{uncorrected} > 0.05$, Table 3).

Table 4 reports the descriptive statistics of the left and right thalamic ROI DTI metrics. No statistically significant differences were found between MO patients and HCs in any of the considered thalamic diffusive metrics ($p_{uncorrected} > 0.05$).

Finally, no significant relationships emerged between interictal photophobia scores and left and right thalamic ROI DTI metrics ($p_{uncorrected} > 0.05$, Table 5).

Table 3 General linear model (F; p) values between interictal photophobia score and left and right thalamic subregion volumes

	Left	Right
Lateral geniculate nucleus (LGN)	0.01; 0.914	0.00; 0.976
Pulvinar inferior (PuI)	0.44; 0.517	0.05; 0.831
Pulvinar medial (PuM)	0.82; 0.380	0.14; 0.717
Pulvinar anterior (PuA)	1.33; 0.267	1.60; 0.225
Pulvinar lateral (PuL)	0.66; 0.429	0.01; 0.936
Whole thalamus	3.55; 0.079	0.60; 0.451

Discussion

The principal finding of this study is the absence of a significant association between perceived photophobia during the interictal phase and either thalamic volume, both overall and within the lateral geniculate nuclei and pulvinar subnuclei, or whole-thalamus microstructural integrity, as assessed by DTI. Given the limited sample size, however, these null findings should be interpreted cautiously, as they may reflect insufficient statistical power rather than a genuine lack of association. Overall, our results indicate that interictal light sensitivity is not associated with detectable macro- or microstructural alterations in the thalamus or in the visual thalamic nuclei examined.

By focusing specifically on the relationship between thalamic structure and subjective interictal photophobia, this study extends previous morphometric research beyond group-level comparisons and addresses a symptom-specific dimension that has not been investigated previously.

Table 2 Mean volumes (mm^3) ± standard deviations, 95% confidence intervals, medians and interquartile ranges (25th–75th percentile) of thalamic subunits and total right and left thalamus in 20 patients with episodic migraine without aura (MO) and 20 healthy controls (HCs). Results from general linear models (GLMs) assessing between-group differences are reported

	Left			Right		
	HCs	MO	Inferential statistics	HCs	MO	Inferential statistics
Lateral geniculate nucleus (LGN)	304.81 ± 52.77 286.6; 270.19–342.93	264.4 ± 44.9 267.3; 229.8–310.1	F = 0.76; p = 0.39 η2 = 0.021	304.77 ± 45.60 287.9; 268.98–334.25	275.0 ± 50.6 257.7; 244.3–310.4	F = 0.06; p = 0.81 η2 = 0.002
Pulvinar inferior (PuI)	258.15 ± 50.21 254.2; 213.93–295.78	236.45 ± 42.51 241.79; 201.37–266.20	F = 2.96; p = 0.09 η2 = 0.078	287.71 ± 56.17 270.8; 241.56–328.45	259.43 ± 41.13 246.43; 231.49–287.72	F = 0.57; p = 0.46 η2 = 0.006
Pulvinar medial (PuM)	1181.50 ± 185.27 1122.5; 1016.70–1284.45	1105.4 ± 150.4 1155.2; 971.9–1235.7	F = 2.16; p = 0.15 η2 = 0.058	1300.82 ± 201.51 1262.9; 1119.74–1461.13	1199.3 ± 147.8 1182.0; 1073.5–1316.5	F = 0.83; p = 0.37 η2 = 0.023
Pulvinar anterior (PuA)	246.60 ± 40.66 237.65; 223.51–271.38	229.24 ± 31.42 236.17; 203.7–256.4	F = 1.85; p = 0.18 η2 = 0.050	260.87 ± 38.70 260.88; 226.02–287.91	244.28 ± 32.02 242.93; 219.14–270.55	F = 1.37; p = 0.25 η2 = 0.038
Pulvinar lateral (PuL)	205.99 ± 48.33 208.5; 161.67–248.88	189.81 ± 38.30 191.52; 153.21–223.64	F = 1.80; p = 0.188 η2 = 0.049	217.01 ± 52.24 217.5; 177.49–250.18	199.05 ± 34.69 190.16; 172.83–209.91	F = 0.98; p = 0.33 η2 = 0.027
Whole thalamus	7527 ± 1286 7123; 6527–8285	6821 ± 830 6792; 6327–7608	F = 0.21; p = 0.65 η2 = 0.006	7775 ± 1184 7764; 6717–8508	7153 ± 903 7016; 6438–7763	F = 0.46; p = 0.50 η2 = 0.013

Table 4 Mean values of each DTI metric (mm^3) ± standard deviations, medians and interquartile ranges (25th–75th percentile) of total right and left thalamus in patients with episodic migraine without aura (MO) and healthy controls (HCs). Results from general linear models (GLMs) assessing between-group differences are reported

	Left			Right		
	HCs	MO	Inferential statistics	HCs	MO	Inferential statistics
FA	0.299 ± 0.017 0.294; 0.275–0.305	0.292 ± 0.017 0.294; 0.275–0.305	F = 0.12; p = 0.731 η2 = 0.004	0.300 ± 0.018 0.296; 0.288–0.315	0.292 ± 0.017 0.292; 0.287–0.305	F = 0.05; p = 0.823 η2 = 0.002
MD	9.16E-4 ± 1.13E-4 8.15E-4; 7.93E-4–8.65E-4	8.77E-4 ± 6.9E-5 8.15E-4; 7.71E-4–8.65E-4	F = 2.22; p = 0.146 η2 = 0.057	8.85E-4 ± 8.8E-5 8.22E-4; 7.56E-4–8.52E-4	8.68E-4 ± 9.00E-5 8.22E-4; 7.56E-4–8.52E-4	F = 0.41; p = 0.527 η2 = 0.003

Table 5 General linear model (F; p) between interictal photophobia score and left, right FA, MD whole thalamus values

	F; p
FAthalamus right	2.34; 0.145
FA thalamus left	0.24; 0.633
MD thalamus right	1.68; 0.213
MD thalamus left	1.45; 0.246

Although photophobia occurs in several clinical conditions, the cerebral mechanisms underlying this symptom remain incompletely understood.

Several lines of evidence support a link between the trigeminovascular system and the visual system in the development of photophobia [2]. Anatomically, second-order neurones from the spinal trigeminal nucleus project to the posterior thalamus, encompassing the pulvinar [9, 11, 34]. Indeed, outside migraine, photophobia is also a common symptom in both meningitis and subarachnoid haemorrhage [35], both conditions with involvement of the meninges. Additionally, it should be noted that the integrity of the visual system is not strictly essential for the perception of light discomfort, as blind individuals can still report this sensation [35].

In line with this, in a previous study, some authors found no differences in the retinal cone visual pathway (both M-L cones and S-cone systems) between healthy controls and subjects with migraine with and without aura recorded during the interictal phase. Additionally, no correlation emerged with subjective discomfort to environmental light exposure [36], suggesting that the retinal cone visual pathway does not play a direct role in interictal photophobia.

Some authors have hypothesized a direct link between the retina and the trigeminal system, as well as an indirect pathway via the dilatation of the choroidal arteries [2]. These alternative pathways include the non-image-producing pathway, which involves the activation of retinal ganglion cells [37], whose axons transmit signals to the visual cortices through the optic nerve, the lateral geniculate nucleus, and the pulvinar in the posterior thalamus [38]. They proposed that the aggravation of migraine headache by light is mediated by photic signals relayed from the retina through the optic nerve to central neurones that process nociceptive signals from the meninges and to hypothalamic nuclei, including the suprachiasmatic nucleus, which play a role in regulating autonomic functions and emotions [39]. Case findings indicate that the pulvinar exhibited markedly enhanced bilateral activation during photophobia [10, 11], and photophobia has been seen in individuals with demyelinating lesions affecting the posterior thalamus [40]. However, hypermetabolism of the posterior thalamus has been documented in individuals with essential blepharospasm, another condition associated with photophobia [41]. Notwithstanding this evidence, our study's results indicate that in our small cohort of patients the degree of interictal photophobia is unrelated to these macro- and micro-structural metrics of the thalamus. Negative structural MRI findings do not preclude the presence of clinically relevant brain alterations. Conventional MRI sequences have limited sensitivity in detecting microstructural abnormalities, diffuse connectivity disruptions, or compensatory functional mechanisms that may occur without overt morphological changes [42]. In this context, volumetric approaches also present important constraints: their ability to detect subtle variations is limited by relatively high detection thresholds, reliance on standardized segmentation models and atlases, and potential spatial normalization errors [43, 44]. Moreover, conventional volumetric measures only partially capture the functional and dynamic organization of neural networks, reducing their interpretive value in conditions characterized primarily by network-level dysfunction rather than tissue loss [45]. More advanced imaging analytics can uncover subtle patterns beyond conventional volumetry and may support the authors' call for future multimodal approaches [46, 47]. Consequently, negative or inconclusive structural results should be interpreted with caution and, when appropriate, complemented by imaging modalities capable of probing microstructural or functional properties beyond the reach of morphometric analysis [46, 47].

In fact, our results do not rule out the involvement of the thalamic nuclei in migraine photophobia from a metabolic and/or functional point of view. Suzuki et al. [48] found that the bilateral thalamus had hypermetabolism in patients with migraine who experience interictal photophobia compared to patients who do not. However, it is important to note that the authors did not grade the level of photophobia. Another study using functional MRI in response to visual stimuli found no significant relationship between the interictal blood oxygen level dependent (BOLD) response of the lateral geniculate nuclei and the level of visual discomfort in patients with both migraine with and without aura [49]. During photophobia, a distinct functional activation pattern was observed in the ventroposteromedial thalamus alongside the trigeminal system [34].

In addition to the thalamus, substantial evidence indicates functional cortical involvement, encompassing both visual and sensorimotor aspects, in the pathophysiology of photophobia during the pericritical phase of migraine. Electrophysiological evidence indicates a negative correlation between subjective photophobia levels and the amplitude of the electroencephalographic response to intermittent photic stimulation [50], as well as with post-movement beta event-related synchronization, which reflects post-activation excitability in the sensorimotor cortices [51]. Consequently, we cannot rule out that other areas of the brain besides the direct visual pathway may play a role in the pathophysiology of photophobia.

Our study has some limitations. These include the small sample size, which substantially limits the interpretability and generalizability of the results. Consequently, the absence of significant correlations should be interpreted with great caution, as it may simply reflect insufficient statistical power rather than a true lack of association. The application of a subjective photophobia rating scale may pose an additional limitation. However, no objective and validated, multidimensional measures of photophobia exist to date. Another limitation of the study is the subjective and retrospective nature of the photophobia rating. It should also be investigated whether other thalamic nuclei, in addition to those analysed, might show associations with photophobia. Additionally, the inclusion of patients without aura only during the interictal phase limits the generalizability of our results to other migraine phases, as well as to patients with migraine with aura.

Furthermore, the migraine cohort comprised patients with relatively low overall disease severity and a limited attack frequency. Because structural and functional brain alterations may be more pronounced in patients with more severe or frequent migraine, the present findings may not be generalizable to the broader migraine population, particularly to individuals with a higher disease burden.

Conclusions

Our study found no evidence of an association between the subjective experience of photophobia and both the volumetric measures of the visual thalamic nuclei and structural integrity of the whole thalamus during the interictal phase of migraine. Our findings indicate that interictal photophobia in migraine is associated with no detectable thalamic structural alterations, although functional or microstructural mechanisms cannot be excluded. Future research should investigate whether this phenomenon also occurs during the presence of an aura and at other phases of the migraine cycle.

Acknowledgements The contribution of the G.B. Bietti Foundation to this paper was supported by the Italian Ministry of Health and Fondazione Roma.

Author contributions Conceptualization, G.C. and F.Car.; methodology, A.D.R.; software, A.D.R. and A.P.; formal analysis, A.D.R. and L.Z.; investigation, G.S., D.C., G.G., F.Cas., C.A., and I.G.; data curation, M.S.; writing—original draft preparation, G.C.; writing—review and editing, G.S., L.Z., and V.P.; supervision, M.A. All authors have read and agreed to the published version of the manuscript.

Funding The authors did not receive funding for the design of the study and collection, analysis, and interpretation of data and in writing the manuscript.

Data availability The informed consent signed by all participants in this study did not include a provision stating that individual raw data can be made publicly accessible. Therefore, in agreement with the Italian data protection law, individual de-identified participant raw data cannot be shared publicly. Researchers meeting the criteria for access to confidential data may access the data upon request, involving the documentation of data access.

Declarations

Ethics approval This study was performed in line with the principles of the Declaration of Helsinki. All the participants provided written informed consent to participate in the study, which was approved by the ethical review board of the Faculty of Medicine at the University of Rome, Italy (N° 0295/2023, March 23, 2023).

Competing interests The authors declare no conflicts of interest directly or indirectly related to the present study.

References

1. Ashina M (2020) Migraine. N Engl J Med 383:1866–1876. https://doi.org/10.1056/NEJMRA1915327
2. Digre KB, Brennan KC (2012) Shedding light on photophobia. J neuro-ophthalmology: official J North Am Neuro-Ophthalmology Soc 32:68–81
3. Headache Classification Committee of the International Headache Society (IHS) (2018) The International Classification of Headache Disorders, 3rd edition. Cephalalgia 38:1–211. https://doi.org/10.1177/0333102417738202

4. Main A, Dowson A, Gross M (1997) Photophobia and phonophobia in migraineurs between attacks. Headache 37:492–495. https://doi.org/10.1046/j.1526-4610.1997.3708492.x
5. Cucchiara B, Datta R, Aguirre GK et al (2015) Measurement of visual sensitivity in migraine: Validation of two scales and correlation with visual cortex activation. Cephalalgia: Int J headache 35:585–592. https://doi.org/10.1177/0333102414547782
6. Boulloche N, Denuelle M, Payoux P et al (2010) Photophobia in migraine: an interictal PET study of cortical hyperexcitability and its modulation by pain. J Neurol Neurosurg Psychiatry 81:978–984
7. Chong CD, Starling AJ, Schwedt TJ (2016) Interictal photosensitivity associates with altered brain structure in patients with episodic migraine. Cephalalgia: Int J headache 36:526–533. https://doi.org/10.1177/0333102415606080
8. Mason BN, Kaiser EA, Kuburas A et al (2017) Induction of Migraine-Like Photophobic Behavior in Mice by Both Peripheral and Central CGRP Mechanisms. J Neurosci 37:204–216. https://doi.org/10.1523/JNEUROSCI.2967-16.2016
9. Noseda R, Kainz V, Jakubowski M et al (2010) A neural mechanism for exacerbation of headache by light. Nat Neurosci 13:239–245
10. Rosini F, Cerase A, Pretegiani E et al (2013) Photophobia and bilateral pulvinar involvement in non-alcoholic Wernicke's encephalopathy. Neurol Sci 34:1867–1869. https://doi.org/10.1007/s10072-013-1338-4
11. Panorgias A, Lee D, Silva KE et al (2019) Blue light activates pulvinar nuclei in longstanding idiopathic photophobia: A case report. Neuroimage Clin 24:102096. https://doi.org/10.1016/j.nicl.2019.102096
12. Noseda R, Burstein R (2011) Advances in understanding the mechanisms of migraine-type photophobia. Curr Opin Neurol 24:197–202. https://doi.org/10.1097/WCO.0b013e3283466c8e
13. Okamoto K, Tashiro A, Chang Z, Bereiter DA (2010) Bright light activates a trigeminal nociceptive pathway. Pain. https://doi.org/10.1016/j.pain.2010.02.004
14. Iglesias JE, Insausti R, Lerma-Usabiaga G et al (2018) A probabilistic atlas of the human thalamic nuclei combining ex vivo MRI and histology. NeuroImage 183:314–326. https://doi.org/10.1016/j.neuroimage.2018.08.012
15. Giardina I, Di Renzo A, Chiffi D et al (2025) 3T MRI thalamic segmentation reveals no macrostructural changes in interictal episodic migraine without aura compared to healthy controls. J Headache Pain 26:243. https://doi.org/10.1186/s10194-025-02196-9
16. Woolrich MW, Jbabdi S, Patenaude B et al (2009) Bayesian analysis of neuroimaging data in FSL. NeuroImage 45. https://doi.org/10.1016/j.neuroimage.2008.10.055
17. Smith SM, Jenkinson M, Woolrich MW et al (2004) Advances in functional and structural MR image analysis and implementation as FSL. NeuroImage 23(Suppl 1):S208–S219. https://doi.org/10.1016/j.neuroimage.2004.07.051
18. Jenkinson M, Beckmann CF, Behrens TEJ et al (2012) FSL NeuroImage 62:782–790. https://doi.org/10.1016/j.neuroimage.2011.09.015
19. Andersson JLR, Skare S, Ashburner J (2003) How to correct susceptibility distortions in spin-echo echo-planar images: Application to diffusion tensor imaging. NeuroImage 20:870–888. https://doi.org/10.1016/S1053-8119(03)00336-7
20. Smith SM (2002) Fast robust automated brain extraction. Hum Brain Mapp 17:143–155. https://doi.org/10.1002/hbm.10062
21. Andersson JLR, Sotiropoulos SN (2016) An integrated approach to correction for off-resonance effects and subject movement in diffusion MR imaging. NeuroImage 125:1063–1078. https://doi.org/10.1016/j.neuroimage.2015.10.019
22. Bastiani M, Cottaar M, Fitzgibbon SP et al (2019) Automated quality control for within and between studies diffusion MRI data using a non-parametric framework for movement and distortion correction. NeuroImage 184:801–812. https://doi.org/10.1016/j.neuroimage.2018.09.073
23. Jenkinson M, Bannister P, Brady M, Smith S (2002) Improved optimization for the robust and accurate linear registration and motion correction of brain images. NeuroImage 17:825–841. https://doi.org/10.1016/S1053-8119(02)91132-8
24. Andersson JLR, Jenkinson M, Smith S (2007) Non-linear registration aka Spatial normalisation FMRIB Technial Report TR07JA2
25. Chong CD, Aguilar M, Schwedt TJ (2020) Altered Hypothalamic Region Covariance in Migraine and Cluster Headache: A Structural MRI Study. Headache 60:553–563. https://doi.org/10.1111/head.13742
26. Reuter M, Rosas HD, Fischl B (2010) Highly accurate inverse consistent registration: a robust approach. NeuroImage 53:1181–1196. https://doi.org/10.1016/j.neuroimage.2010.07.020
27. Ségonne F, Dale AM, Busa E et al (2004) A hybrid approach to the skull stripping problem in MRI. NeuroImage 22:1060–1075. https://doi.org/10.1016/j.neuroimage.2004.03.032
28. Han X, Jovicich J, Salat D et al (2006) Reliability of MRI-derived measurements of human cerebral cortical thickness: The effects of field strength, scanner upgrade and manufacturer. NeuroImage 32:180–194. https://doi.org/10.1016/j.neuroimage.2006.02.051
29. Fischl B, Salat DH, van der Kouwe AJW et al (2004) Sequence-independent segmentation of magnetic resonance images. NeuroImage 23(Suppl 1):S69–84. https://doi.org/10.1016/j.neuroimage.2004.07.016
30. Fischl B, Sereno MI, Dale AM (1999) Cortical surface-based analysis. II: Inflation, flattening, and a surface-based coordinate system. NeuroImage 9:195–207. https://doi.org/10.1006/nimg.1998.0396
31. Fischl B, Sereno MI, Tootell RB, Dale AM (1999) High-resolution intersubject averaging and a coordinate system for the cortical surface. Hum Brain Mapp 8:272–284. https://doi.org/10.1002/(sici)1097-0193(1999)8:4%3C;272::aid-hbm10%3E;3.0.co;2-4
32. Fischl B, Liu A, Dale AM (2001) Automated manifold surgery: constructing geometrically accurate and topologically correct models of the human cerebral cortex. IEEE Trans Med Imaging 20:70–80. https://doi.org/10.1109/42.906426
33. Fischl B, Dale AM (2000) Measuring the thickness of the human cerebral cortex from magnetic resonance images. Proc Natl Acad Sci U S A 97:11050–11055. https://doi.org/10.1073/pnas.200033797
34. Moulton E, Becerra L, Borsook D (2009) An fMRI case report of photophobia: activation of the trigeminal nociceptive pathway. Pain 145:358–363
35. Amini A, Digre K, Couldwell WT (2006) Photophobia in a blind patient: An alternate visual pathway. Case report. J Neurosurg 105:765–768. https://doi.org/10.3171/jns.2006.105.5.765
36. Casillo F, Di Renzo A, Sebastianelli G et al (2024) Lack of a direct link between macular cones function and photophobia in interictal migraine. Cephalalgia 44:3331024241276501. https://doi.org/10.1177/03331024241276501
37. Matynia A, Parikh S, Chen B et al (2012) Intrinsically photosensitive retinal ganglion cells are the primary but not exclusive circuit for light aversion. Exp Eye Res 105:60–69. https://doi.org/10.1016/j.exer.2012.09.012
38. Maleki N, Becerra L, Upadhyay J et al (2012) Direct optic nerve pulvinar connections defined by diffusion MR tractography in humans: implications for photophobia. Hum Brain Mapp 33:75–88
39. Noseda R, Copenhagen D, Burstein R (2019) Current understanding of photophobia, visual networks and headaches. Cephalalgia 39:1623–1634. https://doi.org/10.1177/0333102418784750
40. Kawasaki A, Borruat F-X (2006) Photophobia associated with a demyelinating lesion of the retrochiasmal visual pathway. Am J Ophthalmol 142:854–856. https://doi.org/10.1016/j.ajo.2006.05.026

41. Emoto H, Suzuki Y, Wakakura M et al (2010) Photophobia in essential blepharospasm–a positron emission tomographic study. Mov Disord 25:433–439. https://doi.org/10.1002/mds.22916
42. Tae W-S, Ham B-J, Pyun S-B, Kim B-J (2025) Current Clinical Applications of Structural MRI in Neurological Disorders. J Clin Neurol 21:277–293. https://doi.org/10.3988/jcn.2025.0185
43. Ashburner J, Friston KJ (2000) Voxel-based morphometry–the methods. NeuroImage 11:805–821. https://doi.org/10.1006/nimg.2000.0582
44. Ridgway GR, Omar R, Ourselin S et al (2009) Issues with threshold masking in voxel-based morphometry of atrophied brains. NeuroImage 44:99–111. https://doi.org/10.1016/j.neuroimage.2008.08.045
45. Alexander AL, Lee JE, Lazar M, Field AS (2007) Diffusion tensor imaging of the brain. Neurotherapeutics: J Am Soc Experimental Neurother 4:316–329
46. Fornito A, Zalesky A, Breakspear M (2015) The connectomics of brain disorders. Nat Rev Neurosci 16:159–172. https://doi.org/10.1038/nrn3901
47. Bassett DS, Sporns O (2017) Network neuroscience. Nat Neurosci 20:353–364. https://doi.org/10.1038/nn.4502
48. Suzuki Y, Kiyosawa M, Wakakura M, Ishii K (2024) Hyperactivity of the medial thalamus in patients with photophobia-associated migraine. Headache 64:1005–1014. https://doi.org/10.1111/head.14785
49. Datta R, Aguirre GK, Hu S et al (2013) Interictal cortical hyperresponsiveness in migraine is directly related to the presence of aura. Cephalalgia: Int J headache 33:365–374
50. Bjørk M, Hagen K, Stovner L, Sand T (2011) Photic EEG-driving responses related to ictal phases and trigger sensitivity in migraine: a longitudinal, controlled study. Cephalalgia 31:444–455. https://doi.org/10.1177/0333102410385582
51. Mykland MS, Bjørk MH, Stjern M, Sand T (2018) Alterations in post-movement beta event related synchronization throughout the migraine cycle: A controlled, longitudinal study. Cephalalgia 38:718–729. https://doi.org/10.1177/0333102417709011

Publisher's note Springer Nature remains neutral with regard to jurisdictional claims in published maps and institutional affiliations.

Springer Nature or its licensor (e.g. a society or other partner) holds exclusive rights to this article under a publishing agreement with the author(s) or other rightsholder(s); author self-archiving of the accepted manuscript version of this article is solely governed by the terms of such publishing agreement and applicable law.